

## Magnetoelectric behavior of domain walls in multiferroic $\text{HoMnO}_3$

Thomas Lottermoser\* and Manfred Fiebig†

Max-Born-Institut, Max-Born-Straße 2A, 12489 Berlin, Germany

(Received 5 July 2004; published 21 December 2004)

Local magnetoelectric interactions are revealed as origins of a recently reported coupling between ferroelectric and antiferromagnetic orders in multiferroic  $\text{HoMnO}_3$ . Temperature and field-dependent topography of the antiferromagnetic domain structure evidences massive formation of “spin-rotation domains” which supplement “spin-reversal domains” in the course of a reorientation of  $\text{Mn}^{3+}$  spins. The corresponding domain walls decrease the local magnetic symmetry, thus allowing magnetoelectric coupling between wall magnetization and ferroelectric polarization which modifies the dielectric function.

DOI: 10.1103/PhysRevB.70.220407

PACS number(s): 75.47.Lx, 42.65.Ky, 75.30.Kz, 75.60.Ch

Discovery of the linear magnetoelectric (ME) effect—induction of a polarization by a magnetic field and of a magnetization by an electric field—created a lot of excitement in the 1960s.<sup>1–3</sup> The crosslink between magnetic and electric properties opened new degrees of freedom for device construction based on the mutual control of magnetic and electric states. Originally, the development of ME switching devices failed due to the general smallness of the effect. At present, however, a startling revival of interest in ME phenomena is observed because composite materials and magnetic ferroelectrics have been discovered as candidate materials for “structural” and “gigantic” ME effects which exceed previously known effects<sup>1</sup> by so many orders of magnitude that they can trigger electric or magnetic phase transitions.<sup>4–9</sup> The push for novel materials with large ME effects is complemented by attempts to understand the physical roots of ME behavior. Up to now modification of sublattice magnetization due to charge displacement within the unit cell,<sup>1</sup> effective coupling between magnetostrictive and piezoelectric thin films,<sup>8</sup> geometrically driven ferroelectricity with accompanying magnetic order,<sup>10</sup> and modification of magnetic superexchange by lattice distortion,<sup>6,9</sup> were identified as mechanisms. This variety indicates that a lot more research is indispensable in order to gain a comprehensive picture of the microscopic origins of the ME effect and, thereby, drive it closer to practical use.

In this Rapid Communication we show that massive formation of domain walls in the course of a temperature or magnetic-field-induced antiferromagnetic phase transition is the origin of pronounced ME coupling. Wall formation is caused by nucleation of spin-rotation domains which supplement the existing spin-reversal domains and are observed by magneto-optical imaging techniques. Microscopically the ME behavior originates in coupling between wall magnetization and ferroelectric polarization which is allowed for the low local symmetry in the walls and enhanced by the multiferroicity of the compound.

Multiferroics are characterized by a coexistence of at least two of the following forms of ordering: (anti)ferromagnetism, ferroelectricity, ferroelasticity.<sup>11</sup> They are prime candidates for ME phase control and switching because ferroic long-range order amplifies the electric and/or magnetic fields in matter which in turn enhances ME contributions to the free energy by orders of magnitude.<sup>4–6,12</sup> Hexagonal

$\text{HoMnO}_3$  is multiferroic with ferroelectric ordering at  $T_C = 875$  K,<sup>13</sup> antiferromagnetic  $\text{Mn}^{3+}$  ordering at  $T_N^{\text{Mn}} = 75$  K,<sup>14</sup> and antiferromagnetic  $\text{Ho}^{3+}$  ordering at  $T_N^{\text{Ho}} = 4.6$  K.<sup>15</sup> Anisotropy confines the  $\text{Mn}^{3+}$  spins to the basal  $xy$  plane where frustration leads to eight possible triangular antiferromagnetic structures whose magnetic symmetries are subgroups of the crystallographic space group  $P6_3cm$  of the ferroelectric phase.<sup>16,17</sup> Recently, pronounced ME behavior was observed<sup>18</sup> in the reentrant phase accompanying the temperature or magnetic-field-induced transition between the magnetic  $P6_3cm$  and  $P\bar{6}_3cm$  phases. This was quite unexpected because the bulk ME effect expressed by  $\vec{P} \propto \hat{\alpha} \vec{B}$  or  $\vec{M} \propto \hat{\alpha}^* \vec{D}$  is forbidden in these phases<sup>1,6</sup> and was experimentally excluded.<sup>19</sup> Here  $\hat{\alpha}$  is the ME tensor coupling the polarization  $\vec{P}$  (magnetization  $\vec{M}$ ) to the magnetic field  $\vec{B}$  (electric field  $\vec{D}$ ) in matter. The authors of Ref. 18 proposed that drastic reduction of magnetic symmetry with canting of the  $\text{Mn}^{3+}$  spins out of the basal  $xy$  plane or modifications of the interaction between ferroelectric and antiferromagnetic domain walls<sup>20,21</sup> might explain the ME coupling. However, they concluded that more work is needed in order to identify the actual mechanism.

We investigated the nature of the ME reentrant phase by magneto-optical second harmonic generation (SHG) which proved to be a powerful probe for magnetic structures and interactions.<sup>22–24</sup> Fundamental light at frequency  $\omega$  is incident on a crystal, inducing an electromagnetic polarization at frequency  $2\omega$  which acts as a source for SHG light emitted from the crystal. The magnetic symmetry determines the polarization  $\vec{P}(2\omega)$  of the SHG wave relative to that of the fundamental wave, so that in turn  $\vec{P}(2\omega)$  reveals the underlying arrangement of  $\text{Mn}^{3+}$  spins. The relation between SHG polarization and  $\text{Mn}^{3+}$  ordering in the multiferroic manganites is tabulated in Refs. 14 and 17. It was found that for fundamental light incident along the hexagonal  $z$  axis with polarization along one of the other principal axes, investigation of the  $x$  and  $y$  polarized contributions  $I_x$  and  $I_y$  to the SHG signal unambiguously reveals the magnetic symmetry. Moreover, the  $x$  and  $y$  components of the Mn spins  $\vec{S}$  in the unit cell can be investigated *separately* because of the simple relation  $I_{x,y}^{1/2} \propto S_{y,x}$  [see Fig. 1(c)].

The  $\text{HoMnO}_3$  crystals were flux grown and prepared into

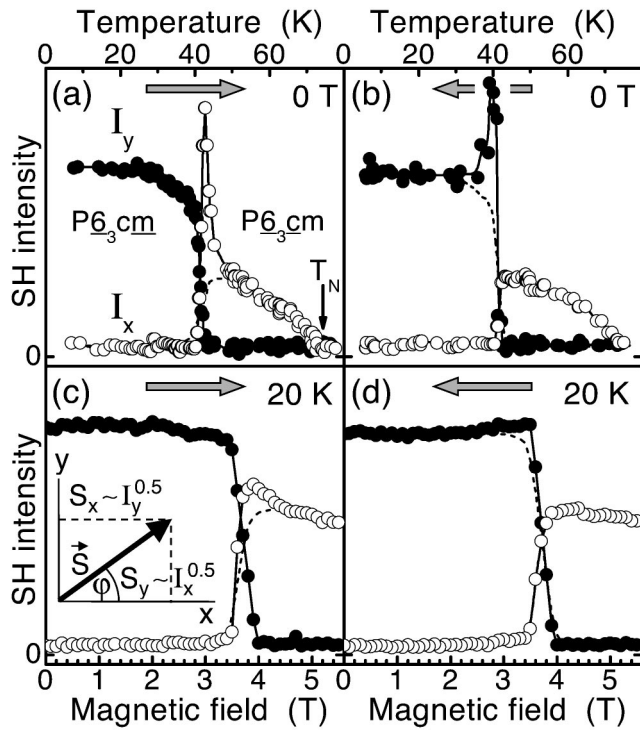


FIG. 1. Temperature and magnetic-field dependence of the intensity  $I_{x/y}$  of  $x/y$ -polarized SHG light from  $\text{HoMnO}_3$ . Fundamental light incident is along the hexagonal  $z$  axis and polarized along one of the principal axes. The gray arrows denote temperature or field scanning directions. The dashed lines show the data for the opposite scanning direction. The inset in (c) depicts the relation between SHG polarization and the vector components of the  $\text{Mn}^{3+}$  spin  $\vec{S}$ .

polished  $z$ -oriented platelets with a thickness of  $\sim 50 \mu\text{m}$ . A transmission set up was used in which the samples were excited with 3-ns light pulses of  $\sim 1 \text{ mJ}$  emitted from an optical parametric oscillator. The polarization was set along the crystallographic  $x$  or  $y$  axis with use of a half-wave plate. In all experiments the photon energy  $2\hbar\omega$  was set to the region of the electronic  ${}^5\Gamma_1 \rightarrow {}^5\Gamma_6$  transitions of  $\text{HoMnO}_3$  at 2.3–2.7 eV, where the largest SHG intensity is observed.<sup>25</sup> Polarization of the SHG light was analyzed with use of a filter or by appropriate choice of photon energy<sup>26</sup> while the fundamental light was suppressed by optical filters. The SHG light was projected onto a cooled charge-coupled device camera by a telephoto lens.

Figure 1 shows the dependence of SHG in  $\text{HoMnO}_3$  on temperature and magnetic field. An  $x$ -polarized SHG signal appears at  $T_N$  whereas at 6 K, the lowest temperature considered in this experiment, the SHG light is  $y$  polarized. Induction of the signal at  $T_N$  confirms its magnetic origin, and in agreement with Fig. 1(c) and Refs. 26 and 27, the  $x$  ( $y$ )-polarized signal corresponds to  $P\bar{6}_3cm$  ( $P\bar{6}_3cm$ ) symmetry with  $\text{Mn}^{3+}$  spins pointing along the  $y$  ( $x$ ) axes. Reorientation of the  $\text{Mn}^{3+}$  spins in zero field occurs at  $T_R=41 \text{ K}$ , which falls well into the range of values between 30–50 K reported by other authors.<sup>14,18,28</sup> In the vicinity of  $T_R$  a remarkable anomaly of the SHG signal is observed. Upon decrease of temperature,  $I_x$  decreases continuously with the progress of the phase transition. However, upon subsequent

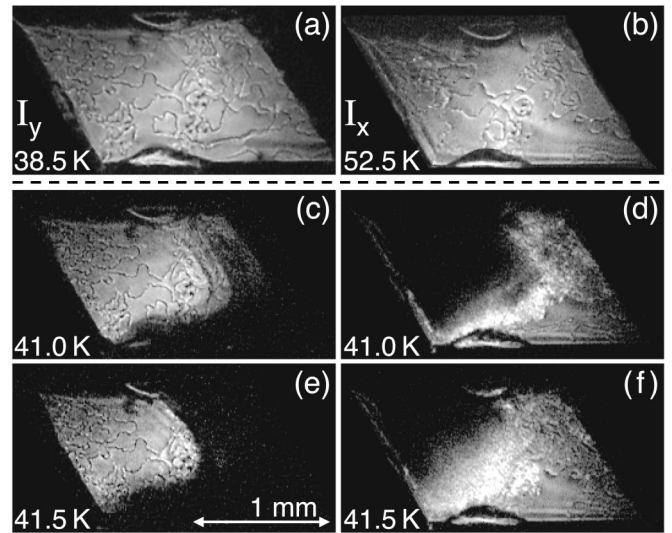


FIG. 2. Antiferromagnetic domain structure of a  $\text{HoMnO}_3$  sample undergoing the magnetic reorientation at  $T_R$  in a temperature increasing run. (a, c, e) Domain structure from  $S_x$  gained with  $y$ -polarized SHG light. (b, d, f) Domain structure from  $S_y$  gained with  $x$ -polarized SHG light. The curvy black lines correspond to domain walls.

increase of temperature,  $I_x$  recovers by passing through a local maximum before the original value of the  $P\bar{6}_3cm$  phase is restored. The envelope describing the maximum has a width of 1–2 K and exceeds the value of the temperature decreasing run by  $\sim 100\%$ . The temperature dependence of  $I_y$  is opposite to that of  $I_x$ .  $I_y$  is quenched upon temperature increase and an additional peaklike contribution to  $I_y$  is observed upon recovery of the  $y$ -polarized SHG signal in the temperature decreasing run. Figures 1(c) and 1(d) show that the magnetic-field dependence of the SHG signal is similar to its temperature dependence. Quenching of the  $y$ -polarized SHG signal below  $T_R$  due to transition into the  $P\bar{6}_3cm$  phase in a static magnetic field along  $z$  occurs as continuous decrease of  $I_y$ , while recovery of the  $P\bar{6}_3cm$  phase is accompanied by the temporary enhancement of SHG intensity. As before, the behavior of  $I_x$  is opposite to that of  $I_y$ . Enhancement of  $I_{x/y}$  occurs in a  $\sim 0.5 \text{ T}$  interval with a maximum enhancement of 10%–30%.

The spatial distribution of  $I_x$  and  $I_y$  on a  $\text{HoMnO}_3$  sample in the vicinity of  $T_R$  is shown in Fig. 2 for a temperature increasing run. At 38.5 K the entire sample is in the  $P\bar{6}_3cm$  phase so that all SHG light is  $y$  polarized. Curvy black lines distributed all over the sample indicate the position of domain walls which separate regions with opposite orientation of corresponding  $\text{Mn}^{3+}$  spins termed “spin-reversal domains.” The black lines are caused by a  $180^\circ$  phase difference and, thus, destructive interference between SHG light fields from neighboring domains.<sup>29,30</sup> Note that in previous work on multiferroic manganites two types of antiferromagnetic domain walls were discovered.<sup>20</sup> Only the so-called “free” antiferromagnetic domains walls which are not clamped to ferroelectric domain walls are discussed and shown in the present work. “Clamped” domain walls are not considered because they were found to be unaffected by all the phase transitions discussed here.

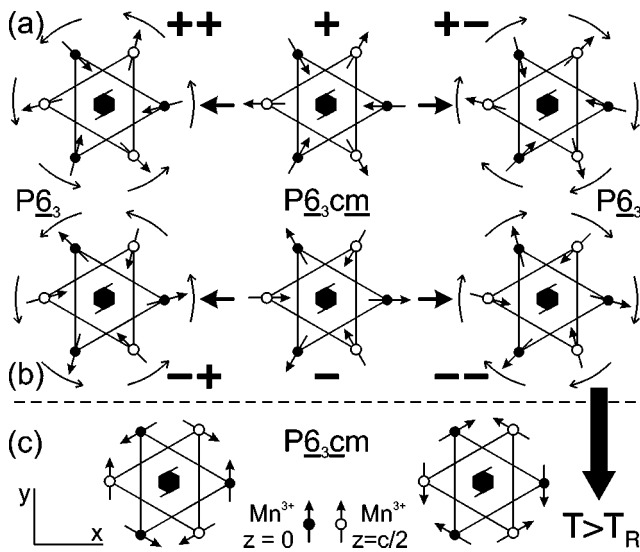


FIG. 3. Domains types in HoMnO<sub>3</sub>. (a, b) Two types of spin-reversal domains of the  $P\bar{6}_3c\bar{m}$  phase (+, -) with associated  $2 \times 2$  spin-rotation domains formed in the  $P\bar{6}_3$  phase by (counter-) clockwise rotation of Mn<sup>3+</sup> spins. (c) Spin-reversal domains of the  $P\bar{6}_3c\bar{m}$  phase reached from (a, b) after completion of the 90° spin rotation in a temperature increasing run (bold arrow).

At 41.0 K the transition to the  $P\bar{6}_3c\bar{m}$  phase is in progress. The sample displays a region on the left-hand side which is still in the  $P\bar{6}_3c\bar{m}$  state ( $I_x=0$ ,  $I_y \neq 0$ ) and a region on the right-hand side where the transition to the  $P\bar{6}_3c\bar{m}$  state has already been completed ( $I_x \neq 0$ ,  $I_y=0$ ). In between these two regions, the reentrant phase with contributions to SHG from both  $I_x \neq 0$  and  $I_y \neq 0$  is observed. At 41.5 K this region has moved further to the left, and at 52.5 K the  $P\bar{6}_3c\bar{m}$  phase has engulfed the whole sample so that only  $x$ -polarized SHG with a distribution of spin-reversal domains different from that in Fig. 2(a) is observed. The inhomogeneity of the phase transition in Fig. 2 and the broad distribution of values reported for the transition temperature<sup>14,18,28</sup> evidences the high sensitivity of  $T_R$  to growth conditions and related compositional gradients.

The unusual enhancement of SHG intensity in the reentrant phase is clearly visible as increase of  $I_x$  in a bright band next to the area with  $I_x=0$  in Figs. 2(d) and 2(f). In this region a grainy distribution of SHG intensity without identifiable domain walls is observed in distinct contrast to the otherwise smooth distribution of SHG intensity in which a network of domain walls creates a three-dimensional effect. A remarkable feature of the reentrant phase is that in spite of the featureless topography of  $I_x$  the  $y$ -polarized component of the SHG signal still displays a well-pronounced distribution of domain walls.

Figure 3 shows a model which explains our observations and reveals the nature of the reentrant phase. The phase transition at  $T_R$  occurs as simultaneous rotation of all Mn<sup>3+</sup> spins between  $\vec{S} \parallel x$  ( $\varphi=0^\circ$ ) in the  $P\bar{6}_3c\bar{m}$  phase and  $\vec{S} \parallel y$  ( $\varphi=90^\circ$ ) in the  $P\bar{6}_3c\bar{m}$  phase. The reentrant phase represents the state with  $0^\circ < \varphi < 90^\circ$  in which the mirror symmetries denoted by  $c$ ,  $\bar{c}$ ,  $m$ ,  $\bar{m}$  are broken so that the resulting symmetry is  $P\bar{6}_3$ . This is unambiguously evidenced by the simul-

taneous presence of contributions with  $I_x \neq 0$  and  $I_y \neq 0$  and the sixfold anisotropy of the SHG signal (not shown). Spin rotation in the  $P\bar{6}_3$  phase can occur as clockwise or counter-clockwise rotation of the magnetic Mn<sup>3+</sup> moments since states at  $-\varphi$  and  $+\varphi$  are energetically equivalent. Physically, this degeneracy corresponds to the formation of two “spin-rotation domains” which supplement the original spin-reversal domains, so that the  $P\bar{6}_3$  phase possesses a total of four types of antiferromagnetic domains which are shown in Fig. 3.

The presence of such spin-rotation domains is evidenced by Figs. 2(e) and 2(f) [as well as Figs. 2(c) and 2(d)]. Figure 2(e) shows the spatial distribution of  $I_y$  and, thus, of the  $x$  component of the Mn<sup>3+</sup> spins. The observed structure is identical to the original distribution of spin-reversal domains in the  $P\bar{6}_3c\bar{m}$  phase at  $T \ll T_R$  even where  $S_x$  and  $I_y$  decrease with increasing value of  $\varphi$ . Rotation of Mn<sup>3+</sup> spins by  $\pm\varphi$  in the reentrant phase corresponds to formation of a component  $\pm S_y$  in the temperature increasing run. Therefore, the spatial distribution of the  $y$  component of the Mn<sup>3+</sup> spins and, thus, of  $I_x$  reflects the spatial distribution of spin-rotation domains. According to Fig. 2(f) their nucleation at  $T_R$  leads to a network of domains with lateral dimensions below the  $\sim 10 \mu\text{m}$  resolution limit of our experiment. The tight network of domains and domain walls explains the grainy distribution of SHG intensity, whereas the enhancement of SHG intensity is due to magnetic gradient effects near the domain walls<sup>31</sup> or constructive interference of SHG from consecutive domains perpendicular to the surface.<sup>30</sup>

Figures 2(d) and 2(f) show that the small rotation domains become unstable in the progress of the spin rotation and collapse finally into the large spin-reversal domains of the  $P\bar{6}_3c\bar{m}$  phase. This newly formed spin-reversal domain structure remains stable up to  $T_N$ . In a temperature or field decreasing run the spin-reversal domains from the  $P\bar{6}_3c\bar{m}$  phase remain stable down to  $I_x=S_y=0$  while nucleation of spin-rotation domains with  $\pm S_x$  occurs so that  $I_y$  displays the enhancement of intensity as evidenced by Figs. 1(b) and 1(d).

In Ref. 18 two different explanations for the increase of the dielectric function  $\hat{\epsilon}$  in the reentrant phase were discussed. (i) First, reduction of magnetic symmetry and/or spin canting along  $z$  were suggested. However, a bulk symmetry lower than  $P\bar{6}_3$  can be excluded on the basis of the polarization dependence of the SHG signal in Fig. 1. Further, only *antiferromagnetic* spin canting along  $z$  is allowed for  $P\bar{6}_3$  symmetry. Even if one assumes that coupling between the ferroelectric polarization and an antiferromagnetic  $z$  component can lead to an uncompensated macroscopic contribution to  $\hat{\epsilon}$ , this contribution was also allowed for  $P\bar{6}_3c\bar{m}$  symmetry and can thus not be restricted to the  $P\bar{6}_3$  phase. (ii) Second, unpinning between ferroelectric and antiferromagnetic domain walls and, thus, a decrease of the number of domain walls in the  $P\bar{6}_3$  reentrant phase, was suggested as being responsible for the increase of  $\hat{\epsilon}$ . This can be excluded on the basis of Fig. 2, which shows that instead of a decrease a drastic increase of wall density occurs in the reentrant phase.

Our data indicate an alternative mechanism for the increase of the dielectric constant in the  $P\bar{6}_3$  state. As shown before<sup>21</sup> antiferromagnetic walls in hexagonal manganites

carry an uncompensated magnetization in the basal  $xy$  plane which reduces the magnetic symmetry within the wall to  $P\bar{2}_1$ . Contrary to the *global*  $P\bar{6}_3$  symmetry of the reentrant phase, the low *local*  $P\bar{2}_1$  symmetry in the walls allows ME contributions  $P_z \propto \alpha_{zx} M_x$  and  $P_z \propto \alpha_{zy} M_y$  which modify the dielectric function. Since the sense of spin rotation in the wall is arbitrary,<sup>21</sup> the sign of the wall magnetization can always accommodate the sign of the ferroelectric polarization so that, independent of the magnetic and electric domain structure, a uniform change of free energy and dielectric function results. The large value of local magnetization and polarization due to multiple long-range ordering enhances the ME effect so that, along with the extreme density of domain walls in the  $P\bar{6}_3$  phase, a pronounced modification of  $\hat{\epsilon}$  is observed.

In summary, massive nucleation of antiferromagnetic do-

main in the course of spin rotation in multiferroic  $\text{HoMnO}_3$  leads to pronounced local ME interactions. The low symmetry in the domain walls allows linear ME coupling between the wall magnetization and the ferroelectric polarization which contributes to the dielectric function. The effect is enhanced by the coexistence of magnetic and electric long-range ordering which is characteristic for multiferroics and demonstrates once more the potential of this class of materials for the generation of unusual or “gigantic”<sup>4–6</sup> ME effects. The result further opens a unique path for generating large ME effects by controlling the local crystallographic and magnetic structure.

The authors thank the DFG for financial support and acknowledge cooperation with R. V. Pisarev, C. Degenhardt, and Th. Lonkai.

\*Present address: Spin Superstructure Project, ERATO, Japan Science and Technology Agency, National Institute of Advanced Industrial Science and Technology, Tsukuba Central 4, Ibaraki 305-8562, Japan.

†Email address: fiebig@mbi-berlin.de

- <sup>1</sup>T. H. O’Dell, *The Electrodynamics of Magneto-Electric Media* (North-Holland, Amsterdam, 1970).
- <sup>2</sup>*Magnetolectric Interaction Phenomena in Crystals*, edited by A. J. Freeman and H. Schmid (Gordon and Breach, London, 1975).
- <sup>3</sup>G. A. Smolenskii and I. E. Chupis, *Sov. Phys. Usp.* **25**, 475 (1982).
- <sup>4</sup>T. Kimura, T. Goto, H. Shintani, K. Ishizaka, T. Arima, and Y. Tokura, *Nature (London)* **426**, 55 (2003).
- <sup>5</sup>N. Hur, S. Park, P. A. Sharma, J. S. Ahn, S. Guha, and S. W. Cheong, *Nature (London)* **429**, 392 (2004).
- <sup>6</sup>Th. Lottermoser, Th. Lonkai, U. Amman, D. Hohlwein, J. Ihringer, and M. Fiebig, *Nature (London)* **430**, 541 (2004).
- <sup>7</sup>C. W. Nan, L. Liu, N. Cai, J. Zhai, Y. Ye, Y. H. Lin, L. J. Dong, and C. X. Xiong, *Appl. Phys. Lett.* **81**, 3831 (2002).
- <sup>8</sup>G. Srinivasan, E. T. Rasmussen, B. J. Levin, and R. Hayes, *Phys. Rev. B* **65**, 134402 (2002).
- <sup>9</sup>M. Fiebig, C. Degenhardt, and R. V. Pisarev, *Phys. Rev. Lett.* **88**, 027203 (2002).
- <sup>10</sup>B. B. Van Aken, T. T. M. Palstra, A. Filippetti, and N. A. Spaldin, *Nat. Mater.* **3**, 164 (2004).
- <sup>11</sup>H. Schmid, in *Magnetolectric Interaction Phenomena in Crystals*, edited by M. Fiebig, V. V. Eremanko, and I. E. Chupis (Springer, Heidelberg, 2004), p. 1.
- <sup>12</sup>H. Schmid, *Ferroelectrics* **161**, 1 (1994).
- <sup>13</sup>P. Coeuré, F. Guinet, J. C. Peuzin, G. Buisson, and E. F. Bertaut, in *Proceedings of the International Meeting on Ferroelectricity*, edited by V. Dvorák (Institute of Physics of the Czechoslovak Academy of Sciences, Prague, 1966), p. 332.
- <sup>14</sup>M. Fiebig, D. Fröhlich, K. Kohn, S. Leute, Th. Lottermoser, V. V. Pavlov, and R. V. Pisarev, *Phys. Rev. Lett.* **84**, 5620 (2000).

- <sup>15</sup>N. Iwata and K. Kohn, *J. Phys. Soc. Jpn.* **67**, 3318 (1998). (Results for  $\text{ErMnO}_3$  and  $\text{HoMnO}_3$  have to be exchanged.)
- <sup>16</sup>Th. Lonkai, D. G. Tomuta, U. Amann, J. Ihringer, R. W. A. Hendrikx, D. M. Többers, and J. A. Mydosh, *Phys. Rev. B* **69**, 134108 (2004).
- <sup>17</sup>M. Fiebig, Th. Lottermoser, and R. V. Pisarev, *J. Appl. Phys.* **93**, 8194 (2003).
- <sup>18</sup>B. Lorenz, A. P. Litvinchuk, M. M. Gospodinov, and C. W. Chu, *Phys. Rev. Lett.* **92**, 087204 (2004).
- <sup>19</sup>B. B. Van Aken and T. T. M. Palstra, *Phys. Rev. B* **69**, 134113 (2004).
- <sup>20</sup>M. Fiebig, Th. Lottermoser, D. Fröhlich, A. V. Goltsev, and R. V. Pisarev, *Nature (London)* **419**, 818 (2002).
- <sup>21</sup>A. V. Goltsev, R. V. Pisarev, Th. Lottermoser, and M. Fiebig, *Phys. Rev. Lett.* **90**, 177204 (2003).
- <sup>22</sup>*Nonlinear Optics in Metals*, edited by K. H. Bennemann (Clarendon, Oxford, 1998).
- <sup>23</sup>A. Kirilyuk, *J. Phys. D* **35**, R189 (2002).
- <sup>24</sup>M. Fiebig, V. V. Pavlov, and R. V. Pisarev, *J. Opt. Soc. Am. B* (to be published 2005).
- <sup>25</sup>C. Degenhardt, M. Fiebig, D. Fröhlich, Th. Lottermoser, and R. V. Pisarev, *Appl. Phys. B: Lasers Opt.* **B73**, 139 (2001).
- <sup>26</sup>M. Fiebig, C. Degenhardt, and R. V. Pisarev, *J. Appl. Phys.* **91**, 8867 (2002).
- <sup>27</sup>Th. Lonkai, D. Hohlwein, J. Ihringer, and W. Prandl, *Appl. Phys. A: Mater. Sci. Process.* **74**, S843 (2002).
- <sup>28</sup>W. C. Koehler, H. L. Yakel, E. O. Wollan, and J. W. Cable, *Phys. Lett.* **9**, 93 (1964).
- <sup>29</sup>S. Leute, Th. Lottermoser, and D. Fröhlich, *Opt. Lett.* **24**, 1520 (1999).
- <sup>30</sup>M. Fiebig, D. Fröhlich, Th. Lottermoser, and M. Maat, *Phys. Rev. B* **66**, 144102 (2002).
- <sup>31</sup>A. V. Petukhov, I. L. Lyubchanskii, and Th. Rasing, *Phys. Rev. B* **56**, 2680 (1997).